Theory of an absolute instability of a finite-length free-electron laser

P. C. Liewer,* A. T. Lin, and J. M. Dawson
Department of Physics, University of California at Los Angeles, Los Angeles, California 90024
(Received 20 February 1980; revised manuscript received 14 August 1980)

The long-wavelength, backward mode of the free-electron laser is shown theoretically to be absolutely unstable for sufficient system length and applied magnetic-field strength. Finite-length one-dimensional particle simulations also show the mode to be absolutely unstable when the theoretical criteria are satisfied. The broad parameter regime in which a free-electron laser can produce the desired forward-propagating short-wavelength radiation, yet be stable to the backward mode, is calculated.

I. INTRODUCTION AND SUMMARY

In the free-electron laser, coherent electromagnetic radiation is efficiently produced by passing a relativistic electron beam through a static rippled magnetic field. The rippled field (wave number k_0) couples the plasma beam and electromagnetic modes, causing an instability which produces forward propagating (in the beam direction), short-wavelength electromagnetic radiation at $k \simeq 2\gamma^2 k_0$ where $\gamma = [1-(v_b/c)^2]^{-1/2}$ and v_b is the beam velocity. The free-electron laser, which is easily tunable from varying the beam γ, can produce radiation from microwave to visible wavelength and has immediate applications in many areas of science and technology. It is under experimental study at several laboratories including Stanford,[1] TRW,[2] NRL-Columbia,[3] and many experiments are in the planning stages.

In addition to the short-wavelength forward mode, there is also a long-wavelength mode ($k \simeq -\frac{1}{2}k_0$ for $\gamma \gg 1$) which propagates backward, i.e., the group velocity $v_{em} = d\omega/dk$ is opposite the beam velocity. Unlike the short-wavelength mode which is convective in nature, i.e., grows as it propagates along the beam, the backward wave can be absolutely unstable due to an automatic feedback between the radiation and the beam. In this paper, the criteria for this mode to absolutely unstable are derived. The instability occurs for

$$\Gamma_0 L > \frac{\pi}{2}(|v_{em} v_b|)^{1/2}, \tag{1}$$

provided $v_{em} v_b < 0$ where L is the system length, Γ_0 is the infinite system growth rate

$$\Gamma_0 = \frac{\omega_c^2}{8} \frac{(k_{em}+k_0)^2}{k_0^2 \gamma^{7/2}} \frac{\omega_{pe}}{\omega_{em}}, \tag{2}$$

where ω_{em} and k_{em} are the frequency and wave number of the backward mode, $\omega_{pe}^2 = 4\pi n e^2/m$ and $\omega_c = eB/mc$, where m is the electron rest mass and B is the strength of the ripple field. Thus the backward mode is absolutely unstable only if the system is long enough or the rippled field strong enough. Results are also presented from a one-dimensional finite-length relativistic computer simulations which also show the mode to be absolutely unstable provided Eq. (1) is satisfied. This absolute instability has also been observed experimentally.[4]

If the backward mode is absolutely unstable, it will grow to such a size that the beam is disrupted and the laser cannot produce the desired short-wavelength radiation. Thus it is important in the design of new experiments, as well as in the interpretation of existing experiments, to understand when this instability occurs. In this paper, we also present the broad parameter regime (e.g., $\gamma > 3$ for $ck_0 > 2.5\omega_{pe}$) where a system can be designed to be long enough to produce the desired short-wavelength radiation, but be short enough to be stable to the long-wavelength backward mode. For real experimental devices, multidimensional and geometric effects can influence the conditions but will not eliminate the necessity to consider this mode. Finite-length 1D particle simulations which show the short-wavelength mode growing convectively to saturation are presented in a subsequent paper.[5]

The organization of this paper is as follows. In Sec. II, the criteria for the backward mode to be absolutely unstable are derived analytically. In Sec. III, results from a one-dimensional particle simulation code are presented which show the backward mode to be absolutely unstable when the theoretical criteria on length and/or pump strength are satisfied. In Sec. IV, we calculate the parameter regime in which a free-electron laser can be operated so that the forward short-wavelength radiation is produced and yet the system is not unstable to the backward mode. The conclusion of this work is discussed in Sec. V.

II. THEORETICAL CRITERIA

The criteria for the absolute instability of the backward mode, Eq. (1), are derived from the coupled equations describing a free-electron laser

$$\left[\left(\frac{\partial}{\partial t}+v_b\frac{\partial}{\partial x}\right)^2+\frac{\omega_{pe}^2}{\gamma^3}\right]\delta n=\frac{ne^2}{\gamma^4 m^2c^2}\frac{\partial^2}{\partial x^2}(\delta\vec{A}_\perp\cdot\vec{A}_{\perp 0}),$$
$$\left(\frac{\partial^2}{\partial t^2}-c^2\frac{\partial^2}{\partial x^2}+\frac{\omega_{pe}^2}{\gamma}\right)\delta\vec{A}_\perp=\frac{-\omega_{pe}^2}{\gamma}\frac{\delta n}{n}\vec{A}_{\perp 0}, \tag{3}$$

where $\vec{A}_{\perp 0}=-(B/k_0)(\hat{y}\cos k_0x+\hat{z}\sin k_0x)$ is the rippled field vector potential, $\delta n(x,t)$ is the perturbed electron density, and $\delta A_\perp$ is the perturbed magnetic vector potential, where $\perp$ refers to perpendicular to the beam direction $(\vec{v}_b=v_b\hat{x})$. Fourier analyzing Eq. (3) in space and time yields the usual dispersion relation for a free-electron laser for an infinite system

$$D_p(\omega,k)D_{\rm em}(\omega,k-k_0)=\frac{k^2}{k_0^2}\frac{\omega_{pe}^2\omega_c^2}{2\gamma^5}, \tag{4}$$

where $D_p(\omega,k)=(\omega-kv_b)^2-\omega_{pe}^2/\gamma^3$ is the usual dispersion relation for the electrostatic plasma beam modes, and $D_{\rm em}(\omega,k)=\omega^2-c^2k^2-\omega_{pe}^2/\gamma$ is the usual dispersion relation for electromagnetic modes. To lowest order in the coupling constant, solutions to Eq. (4) occur when

$$D_p(\omega,k)=0=D_{\rm em}(\omega,k-k_0), \tag{5}$$

which gives the matching conditions

$$\omega_p=\omega_{\rm em},\quad k_p=k_{\rm em}+k_0, \tag{6}$$

where ω_p,k_p is a solution to the uncoupled plasma beam modes dispersion relation $D_p(\omega_p,k_p)=0$ and, similarly, $D_{\rm em}(\omega_{\rm em},k_{\rm em})=0$. Figure 1 plots the solutions to Eq. (5). The two unstable solutions to the coupled dispersion relation occur approximately at the two intersections, corresponding to the matching conditions, Eq. (16). For $\gamma\gg 1$, the short-wavelength solutions occurs at $k_{\rm em}=k_0(v_b/c)(1-v_b/c)^{-1}$. From Fig. 1, it can be seen that for this solution $(k>k_0)$, both the plasma mode $\omega_p(k)$ and the electromagnetic mode $\omega_{\rm em}(k)$ propagate in the same direction ($d\omega/dk$ is positive for both). However, for the long-wavelength solution $[k_{\rm em}=-k_0(v_b/c)(1+v_b/c)^{-1}\ll k_0$ for $\gamma\gg 1]$, the group velocity of the electromagnetic mode is negative and this propagates in the opposite direction from the plasma mode as can be seen in Fig. 1. The infinite system growth rate Γ_0, defined in Eq. (3), is calculated by iterating around the zero-order solutions to Eqs. (5) and (6). To include the effects of finite system length on the free-electron laser, Eqs. (3) are expanded about the solutions to Eqs. (5) and (6) allowing for a slow variation of the mode in space and in time to allow for both convective and absolute instabilities:

$$\delta n(x,t)=N(x,t)\exp[i(k_px-\omega_pt)]+\text{c.c.},$$
$$\delta\vec{A}_\perp(x,t)=A(x,t)\exp[i(k_{\rm em}x-\omega_{\rm em}t)]+\text{c.c.}, \tag{7}$$

where k_p, $k_{\rm em}$, ω_p, $\omega_{\rm em}$ are again the solutions to Eqs. (5) and (6) and c.c. stands for complex conjugate. Substituting Eqs. (7) in Eq. (3), multiplying by $\exp[-i(k_px-\omega_pt)]$ and averaging over the fast time and space scales of the zero-order solution[6] yields

$$\left(\frac{\partial}{\partial t}+v_{\rm em}\frac{\partial}{\partial x}\right)A^-(x,t)=\frac{i}{2}\frac{B}{k_0}\frac{\omega_{pe}^2}{\omega_{\rm em}n}N(x,t),$$
$$\left(\frac{\partial}{\partial t}+v_b\frac{\partial}{\partial x}\right)N(x,t)=\frac{i}{4}\frac{n\omega_c^2}{Bk_0\gamma^4}\frac{k_p^2}{(\omega_p-k_pV_b)}A^-(x,t), \tag{8}$$

where $A^-=A_y-iA_z$ and $v_{\rm em}=c^2k_{\rm em}/\omega_{\rm em}$ is the group velocity of the electromagnetic mode and v_b is the group velocity of the plasma beam modes. These can be put in the form

$$\left(\frac{\partial}{\partial t}+v_s\frac{\partial}{\partial x}\right)a_s=\Gamma_0a_s, \tag{9}$$

where $\Gamma_0(k)$ is the infinite medium growth rate [Eq. (2)], $a_p=N$ and

$$a_{\rm em}=\Gamma_0A^-\left(-\frac{i}{2}\frac{B\omega_{pe}^2}{k_0n\gamma\omega_{\rm em}}\right).$$

Following Ref. 7, finite effects are included by replacing Γ_0 with $\Gamma(x)$ where

$$\Gamma(x)=\begin{cases}0, & x<0\\ \Gamma_0, & 0<x<L\\ 0, & x>L\end{cases} \tag{10}$$

where L is the system length. Laplace transforming Eq. (9), defining

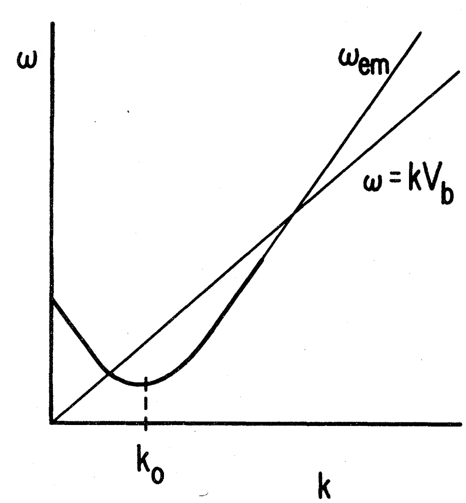

FIG. 1. Graphic solution to the coupled dispersion relation, Eqs. (4) and (5), $\omega_{\rm em}^2=c^2(k-k_0)^2+\omega_{pe}^2/\gamma$ and $(\omega_P-kv_b)^2=\omega_{pe}^2/\gamma^3$. Forward-propagating unstable solution is the intersection at short wavelengths, $k>k_0$. Backward-propagating unstable mode occurs at long-wave-length $(k<k_0)$ intersection.

$$\tilde{a}_s(x,p) = \int dt \exp(-pt) a_s(x,t)$$

and

$$\Psi_s(x,p) = \tilde{a}_s(x,p) \exp\left[\frac{xp}{2}\left(\frac{1}{v_s} + \frac{1}{v_{s'}}\right)\right],$$

yields

$$\frac{\partial^2}{\partial x^2}\Psi_s - \left[\frac{p^2}{4}\left(\frac{1}{v_s} - \frac{1}{v_{s'}}\right)^2 + \frac{\Gamma(x)^2}{v_s' v_{s'}}\right]\Psi_s = \frac{\Gamma_0}{v_s}[\delta(x) - \delta(x-L)]\Psi_{s'} + C_{iv}. \quad (11)$$

where C_{iv} denotes the initial-value contribution. This set of equations (11) has been analyzed by Nishikawa and Liu (Ref. 7) with the results that for absolute instability ($\mathrm{Re}\,p > 0$), a necessary condition is that there be a "potential well" in Eq. (11), i.e., $\Gamma_0^2/v_s v_{s'} < 0$, which implies that $v_p v_{em} < 0$, e.g., the phase velocities of the two coupled modes must be directed oppositely. For most parameters (see also Ref. 8) this condition is satisfied by the backward-mode solution. The dispersion relation is obtained from Eq. (11) by requiring the solutions for $x < 0$ and $x > L$ to vanish at $x = \pm\infty$ and requiring the solution for $0 < x < L$ to be pure oscillatory in space. Matching the solutions at the boundaries and integrating Eq. (11) to obtain the jump condition on the derivations, yields the dispersion relation

$$\tan KL = -K/K_0,$$

where

$$K_0^2 = \frac{p^2}{4}\left(\frac{1}{v_{em}} - \frac{1}{v_b}\right)^2, \qquad K^2 = \Gamma_0^2/|v_{em} v_b| - K_0^2. \quad (12)$$

We obtain the threshold condition for absolute-instability taking $p = 0$ in Eq. (11) and obtain the critical length for instability ($L > L_c$ for instability)

$$L_c = \pi(|v_{em} v_0|)^{1/2}/4\Gamma_0. \quad (13)$$

The critical length for instability L_c is plotted in Fig. 2, normalized to L_c, its asymptotic value for $\gamma \gg 1$,

$$\bar{L}_c = \frac{v_b}{\omega_c} 2\pi^{7/4}\left(\frac{ck_0}{\omega_{pe}}\right)^{1/2}, \quad (14)$$

obtained from the solutions to Eqs. (5) and (6) in the limit $\omega^2 \gg \omega_{pe}^2/\gamma$.

III. SIMULATION RESULTS

One-dimensional finite-length relativistic particle simulations have been performed which verify that the backward mode is absolutely unstable for systems with sufficient length and ripple strength such that $L > L_c$. The code, which is based on that given in Ref. 9, is described in a separate paper.[5] To illustrate the absolute nature of the instability, Fig. 3 shows the longitudinal electric field, E_x at times $\omega_p t = 105$, 115, and 125 from a simulation with $L = 25.6\ v_b/\omega_{pe} = 50/k_0$, $\gamma = 1.9$, $\omega_c = 0.828\omega_{pe}$, and $ck_0 = 2.36\omega_{pe}$. The field E_x grows exponentially in time at each spatial location with the same growth rate $\Gamma = 0.076\omega_{pe}$, and thus the instability is absolute and not convective. The unstable mode had $k_p = 0.7k_0$, in agreement with the backward-mode solution to Eqs. (5) and (6). The theoretical

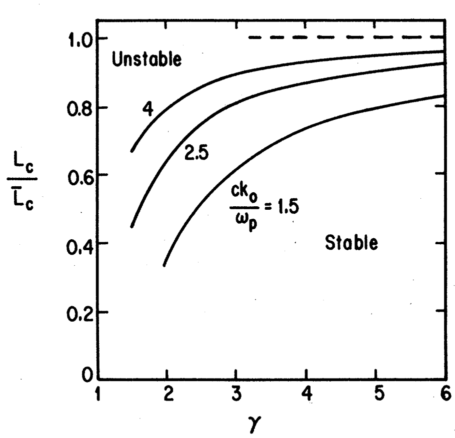

FIG. 2. Critical length for absolute instability of the backward mode, L_c, normalized to its asymptotic value for $\gamma >> 1\bar{L}_c$ (defined in text).

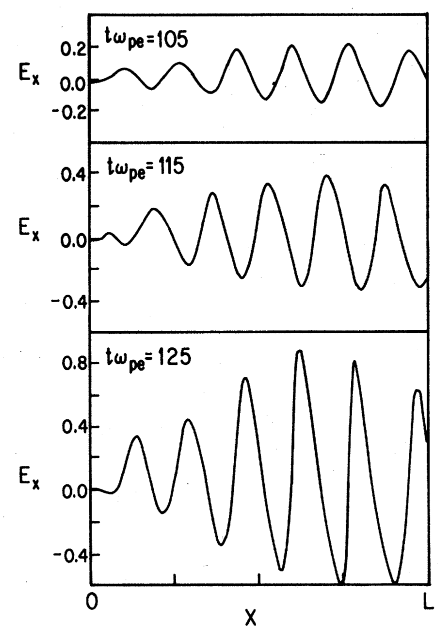

FIG. 3. Longitudinal electric field vs x at time $t\omega_P$ =105, 115, and 125 showing the absolute nature of the instability.

critical length for instability for these parameters is $L_c = 43.5/k_0$, yielding $L = 1.5L_c$ and thus the theory predicts the system to be unstable.

To verify the theoretical threshold further, it is also necessary to show that a system is stable if its length is less than the critical length. Indeed, in another simulation with the same parameters as above, but with half the system length ($L = 25/k_0$), no instability was seen. Since the parameters are the same, the critical length for instability is still $L_c = 43.51k_0$. Thus our simulation verifies that for systems with length less than the critical length, no instability occurs.

Figure 4 plots the tranverse (E_y) and longitudinal (E_x) fields at two instances of time to show that the two modes are, in fact, propagating in opposite directions. The parameters for this simulation were $k_0\Delta x = 0.098$, $L = 1024\Delta x = 100.4/k_0$, $\gamma = 1.6$, $\omega_c = 0.6\omega_{pe}$, and $ck_0/\omega_{pe} = 2.55$. From Fig. 4(a), the wavelength of the transverse mode is calculated to be $k_{em} = 0.23k_0$, which is exactly the theoretically predicted value. The mode is propagating in the negative x direction, opposite the beam, with a phase velocity $v_p/c = -1.7 \pm 0.2$. This is in excellent agreement with the predicted phase velocity for the mode $v_p/c \equiv \omega_{em}/ck_{em} = (c^2k_{em}^2 + \omega_{pe}^2/\gamma)^{1/2}/ck_{em} = -1.66$ [Eq. (5)]. From Fig. 4(b), the wavelength of the plasma mode is calculated to be $k_p = 0.78k_0$ and thus $k_p + k_{em} = 1.01k_0$ and the matching condition is well satisfied. The phase velocity is in the beam direction, as it should be, with $v_p/c = 0.54 \pm 0.04$. This is also in excellent agreement with the theoretical value $v_p/c > \omega_p/ck_p = (kv_b - \omega_{pe}/\gamma^{3/2})/ck_p = 0.52$. The simulation showed these modes to be absolutely unstable with a growth rate $\Gamma = 0.09\omega_{pe}$. The critical length for

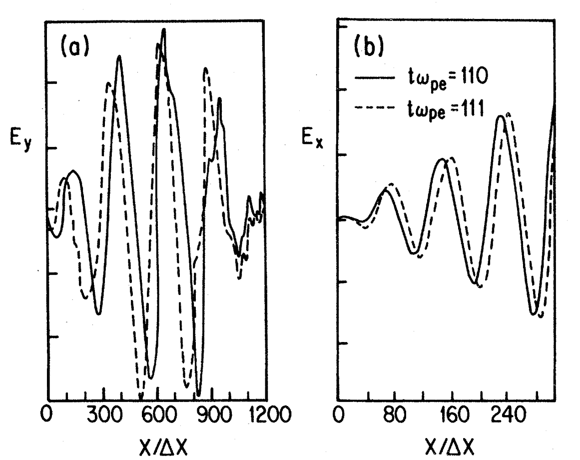

FIG. 4. (a) E_y vs x at $t\omega_{pe} = 110$ and 111 shows backward propagation of electromagnetic mode. (b) E_x vs x at the same times show propagation in beam direction.

absolute instability for these parameters is from Eq. (13), $L_c = 40/k_0$. This is much shorter than the system length $L = 100/k_0$ and so instability was predicted.

IV. PARAMETER REGIME FOR STABLE OPERATION

Because of the great difference in growth rates of the forward and backward modes for large γ, it is possible to design a system which is long enough for the short-wavelength forward mode, which is convectively unstable, to grow to saturation but short enough to be stable to the absolute instability of the backward mode. One-dimensional finite-length simulations have been performed which show that the forward mode grows convectively with growth length $L_G \simeq c/\Gamma_0$, where Γ_0 is the finite system growth length, and saturates by trapping [$k_0L_G \simeq \omega_{pe}/\omega_c(2\gamma^{1/2}ck_0/\omega_{pe})^{3/2}$ for $\gamma \gg 1$]. The results, which are discussed in a separate paper,[5] indicate the mode saturates in roughly 6 or 7 growth lengths. (The backward mode is also observed in these simulations, but because of its small growth rate, it is generally at a low level when the forward mode reaches saturation by trapping. However, if the simulation is continued, the backward mode ultimately grows to such an amplitude that it disrupts the beam, preventing the continued production of the desired mode.) Thus, a free-electron laser should have length $L_f \simeq 7L_G$ to saturate the short-wavelength mode. Therefore a system of length L that satisfies $L_f > L > L_c$ should be able to operate in a steady-state mode. Figure 5 plots γ_c, the critical γ where $L_f(\gamma_c) = L_c(\gamma_c)$ as a function of ck_0/ω_{pe} using Eq. (5) and (6) to calculate Γ_0 for both modes (the criteria are independent of ω_c/ω_{pe}). From the figure one sees that for $ck_0 > 2.5\omega_{pe}$ and $\gamma > 3$, it should be

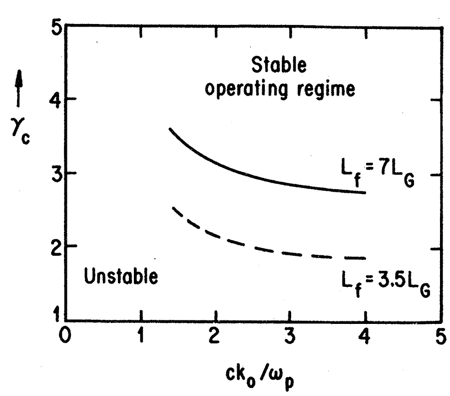

FIG. 5. Plot of the γ at which L_f, the necessary length for a free-electron laser, equals L_c the critical length for absolute instability, L_G is the growth length of the short-wavelength radiation.

possible to operate a free-electron laser in a steady-state mode. It should also be possible to use a free-electron laser as an amplifier. In this case a shorter length than $7L_G$ should suffice. Therefore, for reference, a curve of γ_c for $L_f(\gamma_c) = 3.5L_G(\gamma_c)$ is also shown in Fig. 5.

V. CONCLUSIONS

In conclusion, results from both theory and computer simulations show that for sufficient system length and/or rippled magnetic-field strength, the free-electron laser is absolutely unstable to the long-wavelength ($|k|<|k_0|$), backward-propagating electromagnetic mode. If it is unstable, because of its absolute nature, it will grow to such an amplitude that the system no longer produced the desired short-wavelength radiation. However, there exists a broad parameter regime where one can design a free-electron laser long enough to efficiently produce the short-wavelength radiation, yet short enough to be stable to the absolute instability of the long-wavelength mode. The absolute instability is only a problem when operating the free-electron laser in a steady-state mode. If it is operated for a short time (short time compared to the absolute instability growth time), the short-wavelength mode can still grow and dominate the system because of its much faster growth rate. We also note that a free-electron laser might be designed so that the cavity does not support the long-wavelength mode or selectively absorbs it when multidimensional effects are included. However, its existence must be considered in the design of these devices.

ACKNOWLEDGMENTS

We are happy to acknowledge the numerical support provided by C.-C. Lin. We also thank Dr. Maria Caponi for many fruitful discussions. This work was supported by the NSF under Grant No. PHY 79-01319 and the U. S. Department of Energy under Contract No. DOE De-AM03-76 SF 00010 PA 26, Task III.

*Permanent address: Department of Applied Physics, Caltech, Pasadena, California 91125.

[1]D. A. G. Deacon, L. R. Elias, J. M. J. Madley, G. J. Ramian, H. A. Schwettman, and T. I. Smith, Phys. Rev. Lett. 38, 892 (1977).

[2]H. Bohmer, J. Munch, and M. Z. Caponi, IEEE Trans. Nucl. Sci. NS-26, 3830 (1979).

[3]D. B. McDermott, T. C. Marshall, S. P. Schlesinger, R. K. Parker, and V. L. Granatstein, Phys. Rev. Lett. 41, 1368 (1978).

[4]John Walsh, private communication.

[5]P. C. Liewer, A. T. Lin, J. M. Dawson, and M. Zales Caponi, Phys. Fluids (to be published).

[6]R. Z. Sagdeev and A. A. Galeev, *Nonlinear Plasma Theory* (Benjamin, New York, 1969), Chap. 1.

[7]N. Nishikawa and C. S. Lui, in *Advances in Plasma Physics*, *Vol. 6*, edited by Simon and Thompson (Wiley, New York, 1976).

[8]J. R. Cary and T. J. T. Kwan (unpublished).

[9]T. Kwan, J. M. Dawson, and A. T. Lin, Phys. Fluids 20, 581 (1977).